Journal of Materials Chemistry A

Accepted Manuscript

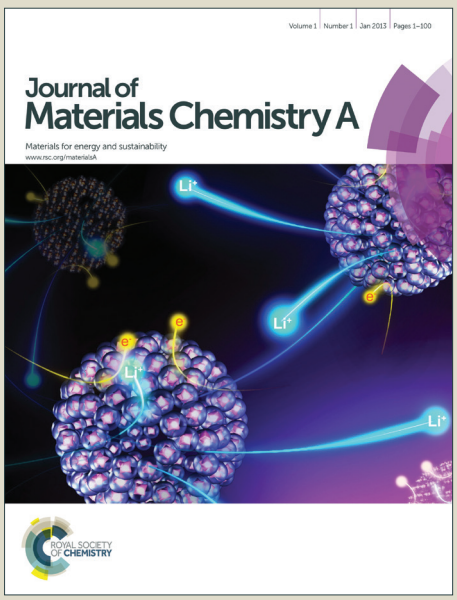

This is an *Accepted Manuscript*, which has been through the Royal Society of Chemistry peer review process and has been accepted for publication.

Accepted Manuscripts are published online shortly after acceptance, before technical editing, formatting and proof reading. Using this free service, authors can make their results available to the community, in citable form, before we publish the edited article. We will replace this *Accepted Manuscript* with the edited and formatted *Advance Article* as soon as it is available.

You can find more information about *Accepted Manuscripts* in the Information for Authors.

Please note that technical editing may introduce minor changes to the text and/or graphics, which may alter content. The journal's standard Terms & Conditions and the Ethical guidelines still apply. In no event shall the Royal Society of Chemistry be held responsible for any errors or omissions in this *Accepted Manuscript* or any consequences arising from the use of any information it contains.

ROYAL SOCIETY OF CHEMISTRY

www.rsc.org/materialsA

Journal Name

ARTICLE

Flexible Supercapacitor Based on Vertically Oriented 'Graphene Forest' Electrodes†

Received 00th January 20xx,
Accepted 00th January 20xx

DOI: 10.1039/x0xx00000x

www.rsc.org/

Yifei Ma,[a,§] Mei Wang,[b,§] Namhun Kim,[a] Jonghwan Suhr[c] and Heeyeop Chae[a,d,*]

Vertically-grown graphene electrodes are developed for flexible electric double layer capacitors (EDLC). Solid-state electrolytes and large area flexible electrodes are essential parts for wearable applications. In this work the vertically-grown graphene electrodes were fabricated by a plasma-enhanced chemical vapor deposition process and applied to flexible electrodes of EDLC. The areal capacitance of the capacitor based on vertical graphene is 2.45 mF/cm^2, which is much better even with solid electrolytes when compared to other reported vertical graphene capacitors. The capacitance also shows good flexibility and it remains unaltered even after 100,000 times of bending or 180 degree folding. These unique features of the capacitor could be ascribed to a discrete 'tree-like' morphology of the vertical graphene, which has not been known before.

Introduction

Graphene, a single layer of graphite, has widely been studied as a carbon-based electrode material for transparent electrode,[1,2] solar cells,[3,4] supercapacitors[5-7] and secondary lithium ion batteries[8,9] due to its high electrical conductivity,[10] high surface area,[11] and excellent mechanical strength.[12] Many processes have been developed to produce graphene for various applications.[13-17]

For supercapacitors, reduced graphene oxide (rGO) obtained from graphene oxide (GO) has mostly been utilized.[8,16,18] The horizontally aligned rGO films, typically used for electrode, however, do not allow easy diffusion of electrolyte ions through the film because of close stacking of rGO sheets.[5,7] To remedy the problem, spacers such as carbon black nanoparticles, carbon spheres, or carbon nanotubes have been inserted into rGO inter-layers.[16,18]

The advent of vertical graphene grown by plasma deposition [19,20] allowed easy and fast access of ions to the electrode without any spacers. This feature of vertical graphene as an electrode, together with the non-porous nature of graphene, made it possible to usher capacitors into the high frequency filtering arena with fast response time.[21-23]

Wearable devices, an emerging technology and a burgeoning trend, require capacitors to power the devices. Because they are worn by human beings, the capacitor has to be safe and furthermore, endure countless number of bending for it to be useful. To satisfy the requirements, a solid electrolyte instead of the usual liquid electrolyte is used. A unique morphological feature of the vertical graphene developed here is utilized to make it utterly unaffected by bending even after 100,000 times of bending.

In this work, we present a wear-tolerant and safe capacitor based on vertical graphene and solid electrolyte. The areal capacitance of the flexible capacitor is higher than that of other vertical-graphene capacitors by an order of magnitude.[23-25] Forest of 'tree-like' vertical graphene grown on quartz substrates is utilized for the electrode, which is termed here vertically oriented graphene forest or simply graphene forest (GF).

Experimental

Preparation of vertically oriented graphene forest:

A 5 × 5 cm^2 quartz substrate was used. It was first cleaned in deionized water and acetone, and blow-dried with N_2 gas. The quartz square was placed in the heating zone of a radio-frequency (RF) plasma enhancement chemical vapor deposition (PECVD) system. The chamber was evacuated to a pressure less than 1 mTorr and then hydrogen gas was introduced at a rate of 8 sccm. After heating the chamber to 850 ℃ and staying at that temperature for 5 min, plasma was generated for 2 min with RF power of 200 W to further remove contaminants on the quartz substrate. Graphene was then grown by introducing C_2H_2 and H_2 at flow rates of 3 sccm and 1 sccm, respectively, for 2 hours with a plasma power of 280 W at a total pressure of 60 mTorr.

Preparation of polymer electrolyte:

[a] School of Chemical Engineering, Sungkyunkwan University(SKKU), Suwon, 440-746, Republic of Korea
[b] Department of Energy Science, Integrated Energy Center for Fostering Global Creative Researcher, Sungkyunkwan University(SKKU), Suwon, 440-746, Republic of Korea
[c] Department of Polymer Science and Engineering, and Department of Energy Science, Sungkyunkwan University(SKKU), Suwon, 440-746, Republic of Korea.
[d] SKKU Advanced Institute of Nanotechnology(SAINT), Sungkyunkwan University(SKKU), Suwon, 440-746, Republic of Korea.
* Email: hchae@skku.edu
§ These author contributed equally to this work.

†.Electronic Supplementary Information (ESI) available: [The XPS survey of GF, stability test of supercapacitor, galvanostatic charge/discharge plots, cyclic voltammetry plots, image of patterned GF/PVA film and table of sheet resistance and atomic concentration of GF.]. See DOI: 10.1039/x0xx00000x

Journal of Materials Chemistry A Accepted Manuscript

Please do not adjust margins

Polyvinyl alcohol (PVA) was utilized to prepare polymer electrolyte. In detail, PVA (98-99% hydrolyzed, medium molecular weight, Alfa Aesar) powder was mixed with water (2 g PVA/20 mL H_2O) and subsequently heated under stirring to around 90 °C in an oil-bath until the solution became clear. After cooling to room temperature, 1.6 g of concentrated phosphoric acid was added to the solution with thorough stirring.

Supercapacitor fabrication and characterization:

The PVA solution thus prepared, 3 ml in volume, was coated on the surface of GF on quartz directly. The coated GF was allowed to dry to form a PVA film. The PVA/GF film was then carefully peeled away from the quartz substrate. The PVA surface is quite sticky and therefore, two pieces of the PVA/GF film can be pasted together easily to form GF/PVA/PVA/GF structure. After GF is peeled away from the quartz, the substrate can be recycled to grow graphene on it again.

The fabricated capacitor was characterized by cyclic voltammetry (CV), galvanostatic charge-discharge (GCD) and electrochemical impedance spectroscopy (EIS). Average specific capacitance can be obtained from CV, GCD, and EIS. For comparison with literature data, the average specific capacitance was calculated from these three characterization results.

The average specific capacitance of GF supercapacitor from the galvanostatic discharge curve was calculated as follows:

$$C = \frac{I}{\Delta V/\Delta t \times a}$$

while the capacity from CV was obtained from,

$$C = \frac{A/2}{s \times \Delta V \times a}$$

where *I, ΔV, Δt, a, s* and *A* are the discharge current, the voltage drop upon discharging, the discharge time, the electrode area, the scan rate, and the integration of positive and negative sweep in cyclic voltammetry curves, respectively.

The specific capacitance of GF supercapacitor from electrochemical impedance spectroscopy was obtained from the following equation:

$$C = \frac{-1}{2 \times \pi \times f \times Z'' \times a}$$

where f is the frequency, Z'' is the corresponding imaginary part of the impedance, and a is the electrode area.

Characterization of materials:

The surface and cross-section morphology of the vertically oriented graphene was examined with field emission scanning electron microscopy (FE-SEM, JEOL, JSM7500F). High-resolution transmission electron microscopy (HRTEM, JEM-2100F JEOL) images were also taken to show successful growth of graphene. Carbon bonding structure was analyzed by Raman spectroscopy (Renishaw, RM-1000 Invia) with a wavelength of 532 nm (Ar^+ ion laser). The sheet resistance of all samples was measured using four-point probe method (Keithley 2420I-V) at room temperature. Cyclic voltammetry (CV), galvanostatic charge-discharge and electrochemical impedance spectroscopy (EIS) were carried out with multichannel potentiostat and galvanostat (Bio-Logic Science Instruments, VMP3). Focused monochromatized Al Kα radiation (hv = 1486.6 eV) was utilized for X-ray photoelectron spectroscopy (XPS, QUANTUM 2000, Physical electronics, USA).

Results and discussion

The graphene was grown in a radio-frequency (RF) plasma-enhanced chemical vapor deposition (PECVD) chamber directly on quartz substrate. For the growth, C_2H_2 and H_2 were introduced to the chamber under vacuum with a RF plasma power applied.

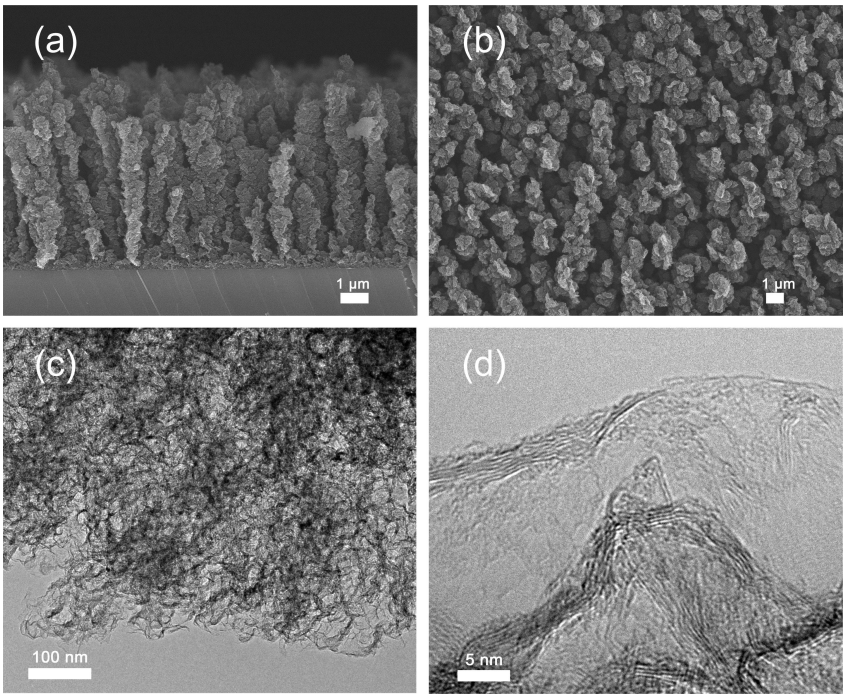

Fig. 1. Morphology of graphene forest (GF): scanning electron microscopy (SEM) images of cross-section (a) and surface (b) on quartz substrate, and detailed structure of GF (c-d) by transmission electron microscopy (TEM) in various magnifications.

Journal of Materials Chemistry A Accepted Manuscript

This journal is © The Royal Society of Chemistry 20xx

Please do not adjust margins

The vertical graphene thus grown exhibited a morphology that is different from any vertical graphene reported so far. The SEM images show detailed morphology of the vertically grown graphene in Fig. 1. From Fig. 1a and 1b, the micrometer scale graphene structure resembles a tree and the packed graphene film looks like a thick forest. The graphene tree is 6.4 μm high on the average and the inter-tree spacing is hundreds of nanometers. Each graphene tree is composed of graphene nanosheets and graphene sheets are seen to be randomly stacked, as confirmed by high-resolution transmission electron microscopy (HR-TEM) images in Fig 1c and 1d. Furthermore, each nanosheet consists of multi-layer graphene instead of single layer graphene (Fig. 1d).

The as-produced GF on quartz substrate shows excellent low sheet resistance of 110 Ω/□. In order to further decrease the resistance, nitric acid treatment is applied, which is one of the effective ways of doping graphene film to increase electric conductivity.[26] The average sheet resistance of GF was decreased by about 12 % to 96 Ω/□ from 110 Ω/□, after doping with concentrated HNO_3 (Table S1). Because of the morphology of GF, the four point probe method only reveals the sheet resistance of bottom horizontal connection for GF, unlike the measurement for mono-layer graphene and other 2D graphene films. However, the doping process takes place to the whole GF film, and therefore, the resistance of the upper part of the film is expected to be decreased. Meanwhile, the SEM images in Fig S2-S3 show that the doping process does not obviously change the vertical nanostructure of GF.

The relation between bonding structure and doping was investigated with Raman spectra as shown in Fig. 2. The vertical graphene in this study is grown on quartz substrates at relatively low temperature of 850°C without any metal catalyst (Cu, Ni, etc.). As a result, the amount of defects is much higher compared to the graphene grown at higher temperature with metal catalyst.[2,26,27] The I_D/I_G ratio increased after the HNO_3 treatment, indicating that the doping process induces defects.[28-30] This result also agrees with XPS results (refer to Fig. S1) and the concentrations of both oxygen and nitrogen increase (Table S1) as a result of the doping.

Fabrication of electric double layer capacitor (EDLC) is rather straightforward when the graphene electrodes are ready as illustrated in Fig. 3. In this work, a generic solid gel electrolyte of PVA/H_3PO_4 was used in fabricating electric double layer capacitors. The method reported by Kaempgen et al.[31] was utilized to prepare the polymer electrolyte. Use of solid electrolyte was motivated by the safety it provides that is needed for wearable devices. Unlike the liquid state electrolyte EDLC, the potential leakage and strict encapsulation can be avoided with the electrolyte bound within the polymer matrix. In this work, the solid electrolyte functions both as a separator and as electrolyte with a single layer structure.

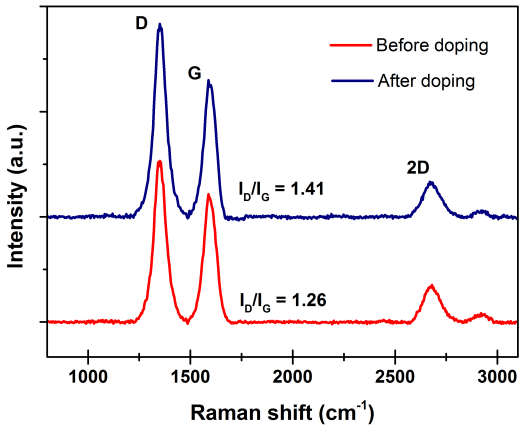

Fig. 2. Raman spectra of GF before (red line) and after (blue line) HNO_3 doping.

After coating the GF with the prepared PVA solution, the coated GF film is allowed to dry to form a PVA/GF film. The PVA/GF film is then carefully peeled away from the quartz substrate. The PVA/GF film is a rubbery flexible film and it also serves as a support film. Owing to the unique rubbery film property, any arbitrary shape of supercapacitor can be realized by simply cutting the film (Fig. S8). The PVA surface is quite sticky and therefore, two pieces of the PVA/GF film can be pasted together easily to form GF/PVA/PVA/GF structure as shown in Fig. 3d. This structure by itself is an electric double layer capacitor when the contact wires are attached. After GF film is peeled from the quartz, the substrate can be recycled to grow graphene on it again. A current collector can be used to enhance the performance of the capacitor (Fig. 3f). One major role of current collector in a capacitor is to collect/transport charge carriers effectively to/from active material during charge and discharge processes.[5] Copper foil was used as the current collector in this work.

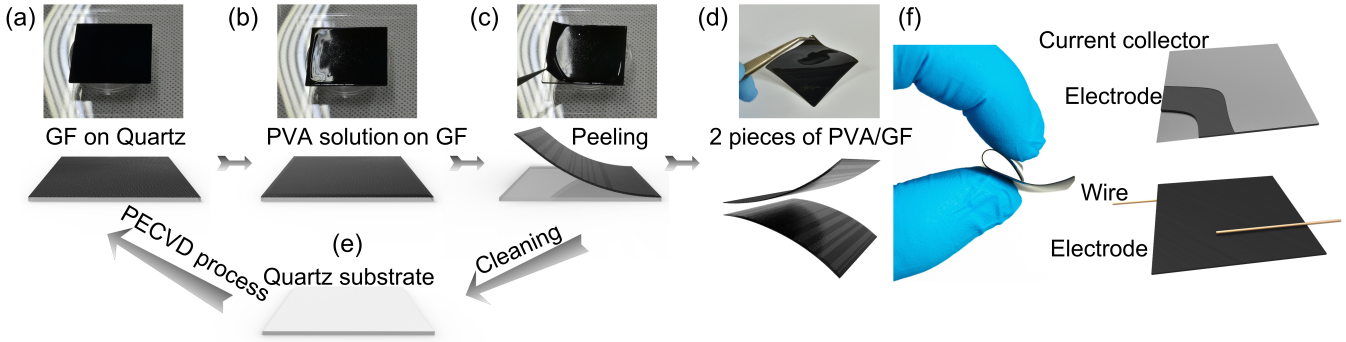

Fig. 3. Schematic illustration of fabrication of flexible GF electrode and that of EDLC. (a) Vertically oriented graphene forest (GF) is grown on quartz substrate. (b) Polyvinyl alcohol (PVA) solution is coated on GF. (c) After PVA film is formed, the PVA/GF is carefully peeled from the substrate. (d) 2 pieces of PVA/GF film are pasted together. (g) The quartz substrate can repeatedly be used for GF growth. (f) EDLCs with and without current collector

Journal of Materials Chemistry A Accepted Manuscript

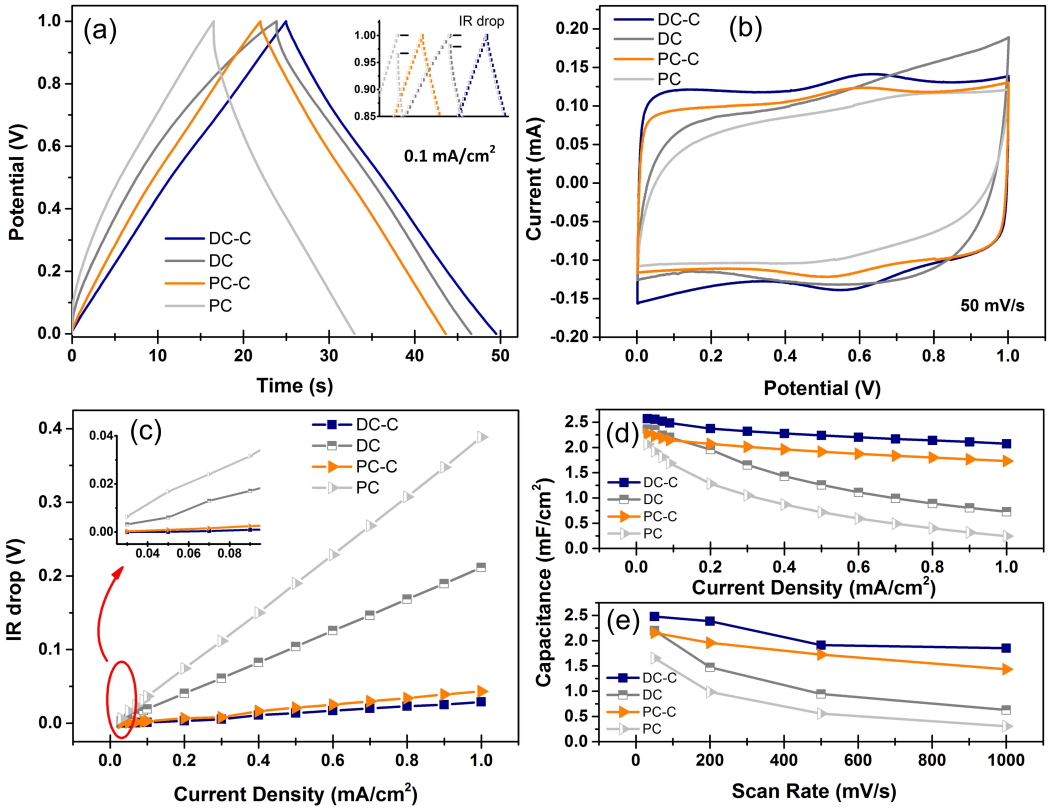

Fig. 4. Electrochemical performance of four types of EDLCs: pristine EDLC (PC), doped EDLC (DC), PC with current collector (PC-C), DC with current collector (DC-C). (a) Galvanostatic charge/discharge plots at current density of 0.1 mA/cm^2. The inset image of (a) shows magnified tips of charge/discharge plots to reveal IR drop. (b) Cyclic voltammetry at 50 mV/s. (c) IR drop of GF-EDLCs as a function of current density. (d) Specific capacitance of GF-EDLCs as affected by current density, and (e) by scan rate.

To ascertain the positive effects of doping and use of current collector, four different types of capacitor were fabricated: pristine GF-EDLC (PC), doped GF-EDLC (DC), PC with current collector (PC-C), and DC with current collector (DC-C). The results of galvanostatic charge/discharge at 0.1 mA/cm^2 and cyclic voltammetry (CV) at 50 mV/s are shown in Fig. 4a and 4b, respectively. The capacitances obtained from Fig. 4a for the four types of capacitor are: 2.45 mF/cm^2 for DC-C, 2.30 mF/cm^2 for PC-C, 2.21 mF/cm^2 for DC, and 1.67 mF/cm^2 for PC. Similar results were obtained for the capacitance calculated from CV (Fig. 4b).

Two findings emerge from the results obtained. While the capacitance is of the same order of magnitude for all the four types, the doped capacitor with current collector (DC-C) yielded the highest capacitance. The other finding that stands out is the fact that the doped capacitor without current collector yields a capacitance fairly close to that of the doped capacitor with current collector, i.e., 2.21 mF/cm^2 for DC vs. 2.45 mF/cm^2 for DC-C. This finding signifies that the GF-EDLC does not necessarily need a current collector, a distinct advantage over the one with metal collector film in terms of cost and flexibility, at least in the low current density region below 0.1 mA/cm^2. It is notable that the beneficial effect of doping is greater for the capacitor without the current collector than with the collector.

The dynamic voltage drop or IR drop given in Fig. 4c for various current densities indicates that the drop in general increases with increasing current density. The IR drop for the EDLCs with current collector (PC-C and DC-C) remains very low even at high current density owing to the low resistance of current collector. However, the IR drop of the EDLCs without current collector (PC and DC) increases quickly when current density increases due to the sheet resistance of GF film that is higher compared to metal. As a consequence, a large amount of energy will be consumed when discharging the EDLCs without current collector at high current density. Nevertheless, for the current density lower than 0.1 mA/cm^2, the IR drop of PC and DC is low enough (less than 0.04 V, as shown in Fig. 4c and inset image) to be useful for low current devices.

Dependence of the capacitance of the EDLCs on current density and scan rate is shown in Fig. 4d and 4e (Fig. S5 and S6 for more detail information), respectively. It is notable that the capacitance of the EDLCs with current collector (PC-C and DC-C) shows a relatively slow decrease with an increase in current density as well as scan rate. However, the EDLCs without the current collector show a sharp decrease in the capacitance because of the amplified resistance of GF film to capacitance at high current density and scan rate. It is notable that the IR drop is low at low current density (less than 0.1 mA/cm^2). So the effect of current collector is insignificant. Therefore, the doped GF based EDLC has a higher capacitance than that of pristine GF based EDLC. As the current density increases, the capacitance of DC decreases faster than that of PC-C due to the higher IR drop of DC (Fig. 4c), resulting in crossover of capacitances of DC and PC-C.

To investigate the kinetic features of ion diffusion, electrochemical impedance spectroscopy (EIS) was carried out. Nyquist plots obtained for the four types of EDLCs in the

Journal of Materials Chemistry A Accepted Manuscript

This journal is © The Royal Society of Chemistry 20xx

Please do not adjust margins

frequency range between 300 kHz and 1 mHz are shown in Fig. 5a with a magnified view of the high-frequency range in Fig. 5b for the capacitors with current collector. The plots show nearly vertical lines for the capacitor with current collector, revealing excellent ion diffusion behavior, whereas the lines for those without the collector are not vertical. The perfect semicircles for the EDLCs with current collector in the high frequency region of the Nyquist plot (Fig.5b) imply porous characteristics of GF.[32] The diameter of semicircle for DC-C is shorter than for PC-C, indicating a lower charge transfer resistance [22] due to doping by HNO_3. The GF-EDLCs with current collector show lower equivalent series resistance (19 Ω for DC-C and 23 Ω for PC-C) in comparison with those without current collector (90 Ω for DC and 130 Ω for PC).

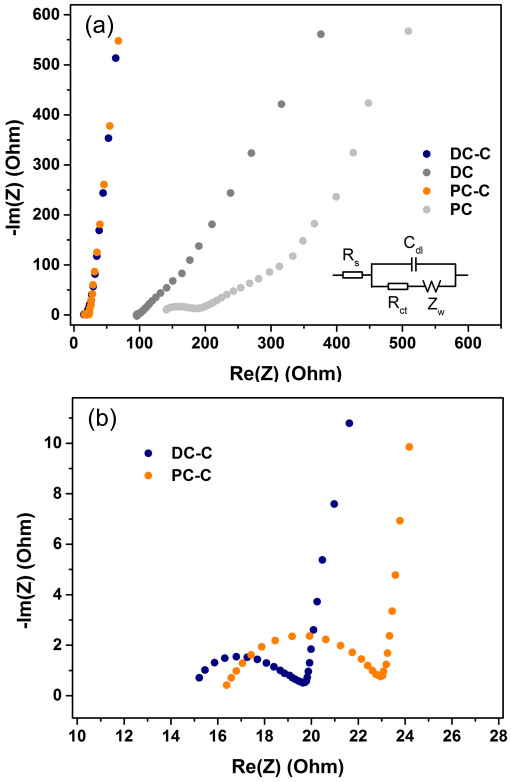

Fig. 5. (a) Nyquist plots of four types of GF-EDLCs and (b) magnified high frequency region plots for GF-EDLCs with current collector. The inset in (a) shows equivalent circuit

Most of the data on the specific capacitance reported for vertical graphene capacitors are at 120 Hz, attainable from EIS, because of interests in high frequency applications. The highest specific capacitance in this work at the frequency was obtained from DC-C, yielding a capacitance of 1.36 mF/cm^2 with 6.4μm high graphene (Fig. S7). In comparison, Sheng et al.[24] reported that electrochemically reduced graphite oxide electrodes gave a specific capacitance of 0.283 mF/cm^2 with 20 μm thick film. Ren et al.[23] fabricated a capacitor with 2 μm thick vertical graphene on a 200 μm Ni foam, producing a specific capacitance of 0.360 mF/cm^2 at 120 Hz. Cai et al.[25] reported a capacitance of 0.265 mF/cm^2 at 120 Hz for the capacitor fabricated with 2 μm thick vertical graphene nanosheets. Liquid electrolytes were used for all these capacitors. While the capacitance depends on the frequency, and applications could be different, the comparison does indicate that the capacity of the flexible capacitor presented here, even with solid electrolyte, is almost an order of magnitude greater compared to the others.

Stability of the device when subjected to repeated charge/discharge cycles is a measure of interest for any capacitor. This stability was tested at the current density of 0.1 mA/cm^2 (Fig. S4) for the four types of the EDLC. The figure shows that there is no significant change during the 10,000 cycles for the EDLCs with current collector. The EDLCs without current collector also show a good capacitance retention but with a little undulation. The undulation could be ascribed to the change of ambient temperature that affects the internal resistance of GF during the measurement, which can be neglected for the ones with current collector.

One aspect of bendability is the extent to which the device can be bent. Another has to do with bending durability. The latter is a measure of device lifetime since repeated bending usually leads to loss of capacitance. As a power supply of wearable devices, this aspect becomes a critical factor because these devices are subject to countless number of bending during their lifetime. For the bendability tests, HNO_3 doped capacitors (DC and DC-C) were used. Fig. 6a shows the retention of the capacitance as a function of bending radius, with the value for the flat capacitor as the reference. The result for DC-C, which is the doped capacitor with current collector, shows that the capacitance improved slightly for bending radii of 12.95 mm, 11.13 mm and 7.59 mm.

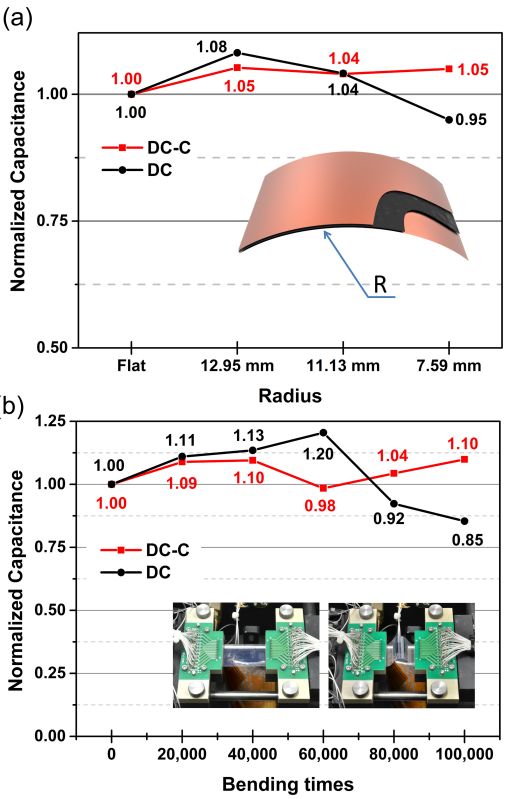

Fig. 6. Flexibility tests of doped GF-EDLC with current collector (DC-C): (a) Capacitance as affected by bending radius. (b) Retention rate of capacitance as affected by times of bending at bending radius of 10 mm.

Journal of Materials Chemistry A Accepted Manuscript

Durability of the device when subjected to repeated bending/flattening was tested with a home-made bending machine, as shown in Fig. 6b. After the capacitor is bent to a radius of 10 mm repeatedly for a specified number of times, the capacitor was flattened and the capacitance was measured. The results in the figure reveal that the capacitor without the current collector does not lose its capacitance even after 80,000 times of bending but then the capacitance deteriorates rather rapidly thereafter on. All the bending experiments reported in the literature involved bending times less than 10,000. Huang et al.[33] and Kou et al.,[34] for instance, reported bending test results only after 5,000 and 1,000 times of bending, respectively.

The finding here indicates that the bending test should perhaps be extended to 100,000 times rather than less than 10,000 times for wearable applications, considering countless number of times of bending such a device has to endure over its lifetime when worn on a person. A unique feature of the capacitor presented here is the device with copper foil current collector shown in Fig. 6b. No deterioration of the capacitance occurred even after 100,000 times of bending (slight decrease of capacitance for DC-C occurred at bending times of 60,000 because of the room temperature change during the long time bending test [35]). This superb bending durability could be ascribed to the nature of the graphene forest in which each graphene tree stands on its own, rather than connected as in the usual vertical graphene structure. Therefore, the bending occurs in between trees rather than against the connected layer of graphene, which would leave the graphene trees intact.

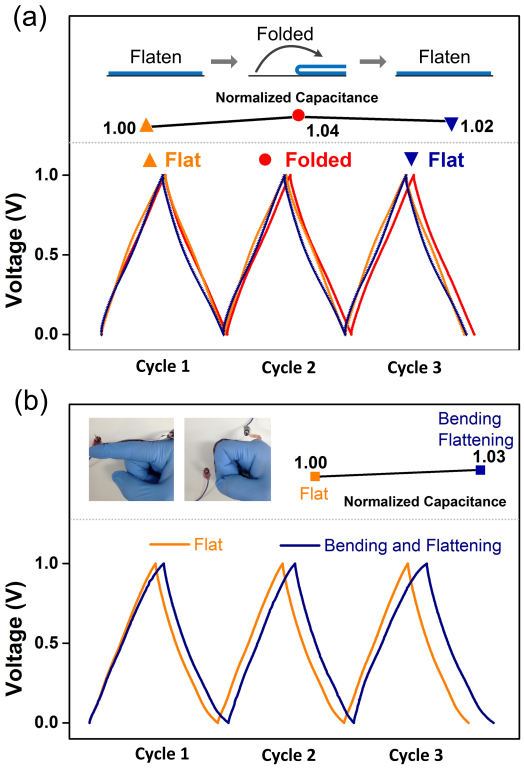

Fig. 7. Plots of normalized capacitance and GCD curves of 180 degree folded DC-C (a) and dynamically bended DC-C (b).

Folding test was performed to investigate the bending limitation as shown in Fig.7a. The DC-C does not show any loss of capacitance even with the 180 degree folding. In order to simulate dynamic operation situation, bending and flattening motion was repeated with the DC-C attached on the finger joint of a glove. The bending frequency is about 1 time per second. Fig. 7b shows that the dynamic bending and flattening dose not decrease the capacitance of DC-C. The folding and bending test show excellent flexibility of the GF based EDLC.

Conclusions

The flexible capacitor presented here should be suitable for wearable devices in terms of safety and bending durability. The unique morphological feature of the vertical graphene in the form of graphene trees, which is introduced here for the first time, has made it possible to produce a capacitor that can withstand 100,000 times of bending or 180 degree folding without any loss of capacity and to provide an areal capacitance that is an order of magnitude larger than any capacitor made with vertical graphene. With the exception of graphene forest, only generic materials are used for the fabrication of the capacitor, and as such the fabrication is cost-effective. The capacitor with graphene forest as the electrode can be used as such without metal current collector, almost without loss of capacitance and IR drop, for low current density applications.

Acknowledgements

This research was supported by the Basic Science Research Program through the National Research Foundation of Korea (NRF) funded by the Ministry of Education, Science and Technology (2011-0006268). This research was also supported by the MKE (The Ministry of Knowledge Economy), Korea, under the ITRC (Information Technology Research Center) support program (NIPA-2012-H0301-12-4013) supervised by the NIPA (National IT Industry Promotion Agency).

Notes and references

1 Y. Guo, L. Lin, S. Zhao, B. Deng, H. Chen, B. Ma, J. Wu, J. Yin, Z. Liu and H. Peng, *Adv. Mater.*, 2015, **27**, 4315-4321.
2 J. Zhang, P. A. Hu, X. N. Wang, Z. L. Wang, D. Q. Liu, B. Yang and W. W. Cao, *J. Mater. Chem.*, 2012, **22**, 18283-18290.
3 O. Vazquez-Mena, J. P. Bosco, O. Ergen, H. I. Rasool, A. Fathalizadeh, M. Tosun, M. Crommie, A. Javey, H. A. Atwater and A. Zettl, *Nano Lett.*, 2014, **14**, 4280-4285.
4 Z. Yin, J. Zhu, Q. He, X. Cao, C. Tan, H. Chen, Q. Yan and H. Zhang, *Adv. Energy Mater.*, 2014, **4**, 1300574.
5 Z. Bo, W. Zhu, W. Ma, Z. Wen, X. Shuai, J. Chen, J. Yan, Z. Wang, K. Cen and X. Feng, *Adv. Mater.*, 2013, **25**, 5799-5806.
6 K. Gao, Z. Shao, J. Li, X. Wang, X. Peng, W. Wang and F. Wang, *J. Mater. Chem. A*, 2013, **1**, 63-67.
7 Y. Yoon, K. Lee, S. Kwon, S. Seo, H. Yoo, S. Kim, Y. Shin, Y. Park, D. Kim, J. Y. Choi and H. Lee, *ACS Nano*, 2014, **8**, 4580-4590.
8 J. Qin, C. He, N. Zhao, Z. Wang, C. Shi, E. Z. Liu and J. Li, *ACS Nano*, 2014, **8**, 1728-1738.

Journal of Materials Chemistry A Accepted Manuscript

This journal is © The Royal Society of Chemistry 20xx

Please do not adjust margins

9 J. Chang, X. Huang, G. Zhou, S. Cui, P. B. Hallac, J. Jiang, P. T. Hurley and J. Chen, *Adv. Mater.*, 2014, **26**, 758-764.
10 S. De and J. N. Coleman, *ACS Nano*, 2010, **4**, 2713-2720.
11 Y. Zhu, S. Murali, M. D. Stoller, K. J. Ganesh, W. Cai, P. J. Ferreira, A. Pirkle, R. M. Wallace, K. A. Cychosz, M. Thommes, D. Su, E. A. Stach and R. S. Ruoff, *Science*, 2011, **332**, 1537-1541.
12 Z. Chen, W. Ren, L. Gao, B. Liu, S. Pei and H. M. Cheng, *Nat. Mater.*, 2011, **10**, 424-428.
13 T. Kobayashi, M. Bando, N. Kimura, K. Shimizu, K. Kadono, N. Umezu, K. Miyahara, S. Hayazaki, S. Nagai, Y. Mizuguchi, Y. Murakami and D. Hobara, *App. Phys. Lett.*, 2013, **102**, 023112.
14 W. Yang, G. Chen, Z. Shi, C. C. Liu, L. Zhang, G. Xie, M. Cheng, D. Wang, R. Yang, D. Shi, K. Watanabe, T. Taniguchi, Y. Yao, Y. Zhang and G. Zhang, *Nat. Mater.*, 2013, **12**, 792-797.
15 A. Delamoreanu, C. Rabot, C. Vallee and A. Zenasni, Carbon, 2014, **66**, 48-56.
16 Z. B. Lei, N. Christov and X. S. Zhao, *Energy Environ. Sci.*, 2011, **4**, 1866-1873.
17 T. Terasawa and K. Saiki, *Carbon*, 2012, **50**, 869-874.
18 G. Wang, X. Sun, F. Lu, H. Sun, M. Yu, W. Jiang, C. Liu and J. Lian, *Small*, 2012, **8**, 452-459.
19 Y. Ma, H. Jang, S. Kim, C. Pang and H. Chae, *Nanoscale Res. Lett.*, 2015, **10**, 1-8.
20 M. Y. Zhu, J. J. Wang, B. C. Holloway, R. A. Outlaw, X. Zhao, K. Hou, V. Shutthanandan and D. M. Manos, *Carbon*, 2007, **45**, 2229-2234.
21 M. Z. Cai, R. A. Outlaw, S. M. Butler and J. R. Miller, *Carbon*, 2012, **50**, 5481-5488.
22 H. Yoo, M. Min, S. Bak, Y. Yoon and H. Lee, *J. Mate. Chem. A*, 2014, **2**, 6663-6668.
23 G. F. Ren, X. Pan, S. Bayne and Z. Y. Fan, *Carbon*, 2014, **71**, 94-101.
24 K. Sheng, Y. Sun, C. Li, W. Yuan and G. Shi, *Sci. Rep.*, 2012, **2**, 247-254.
25 M. Cai, R. A. Outlaw, R. A. Quinlan, D. Premathilake, S. M. Butler and J. R. Miller, *ACS Nano*, 2014, **8**, 5873-5882.
26 S. Bae, H. Kim, Y. Lee, X. Xu, J. S. Park, Y. Zheng, J. Balakrishnan, T. Lei, H. R. Kim, Y. I. Song, Y. J. Kim, K. S. Kim, B. Ozyilmaz, J. H. Ahn, B. H. Hong and S. Iijima, *Nat. Nanotechnol.*, 2010, **5**, 574-578.
27 S. J. Chae, F. Gunes, K. K. Kim, E. S. Kim, G. H. Han, S. M. Kim, H. J. Shin, S. M. Yoon, J. Y. Choi, M. H. Park, C. W. Yang, D. Pribat and Y. H. Lee, *Adv. Mater.*, 2009, **21**, 2328-2333.
28 Z. Q. Luo, C. X. Cong, J. Zhang, Q. H. Xiong and T. Yu, *Carbon*, 2012, **50**, 4252-4258.
29 X. Li, C. W. Magnuson, A. Venugopal, J. An, J. W. Suk, B. Han, M. Borysiak, W. Cai, A. Velamakanni, Y. Zhu, L. Fu, E. M. Vogel, E. Voelkl, L. Colombo and R. S. Ruoff, *Nano Lett.*, 2010, **10**, 4328-4334.
30 A. C. Ferrari and D. M. Basko, *Nat. Nanotechnol.*, 2013, **8**, 235-246.
31 M. Kaempgen, C. K. Chan, J. Ma, Y. Cui and G. Gruner, *Nano Lett.*, 2009, **9**, 1872-1876.
32 J. Lin, C. Zhang, Z. Yan, Y. Zhu, Z. Peng, R. H. Hauge, D. Natelson and J. M. Tour, *Nano Lett.*, 2013, **13**, 72-78.
33 T. Huang, B. Zheng, L. Kou, K. Gopalsamy, Z. Xu, C. Gao, Y. Meng and Z. Wei, *RSC Adv.*, 2013, **3**, 23957-23962.
34 L. Kou, T. Huang, B. Zheng, Y. Han, X. Zhao, K. Gopalsamy, H. Sun and C. Gao, *Nat. Commun.*, 2014, **5,** 3754.
35 M. Wang, L. D. Duong, N. T. Mai, S. Kim, Y. Kim, H. Seo, Y. C. Kim, W. Jang, Y. Lee, J. Suhr and J. D. Nam, *ACS Appl. Mater. Inter.*, 2015, **7**, 1348-1354.

Journal of Materials Chemistry A Accepted Manuscript

Please do not adjust margins

Table of contents

A flexible supercapacitor was demonstrated with ‘graphene forest’ as electrodes. No capacitance loss was observed even with 100,000 time bending.

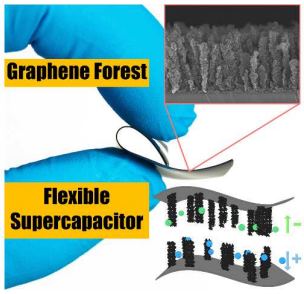

Journal of Materials Chemistry A Accepted Manuscript